Expanded View Figures

A

Multiple sequence alignment of *XBP1* introns in several species of metazoans

```
Drosophila melanogaster      GCGUCCACCAACCUUGGAUCUGCAGCAUCCA---AAGCUGACCCUCUGCCGCAGGGUAUACAACAGGUGGACA
Caenorhabditis elegans       GAUCGCCGUGCCUUUGAAUCAGCAGCAUUCA---UUAAUGAGCCUCAGCAGUGGGAACAGGCCCGAUCCAACA
Canis lupus familiaris       GUGGCCGGGUCUGCUGAGUCCGCAGCACUCAGACUACGUGCAUC--UGCAGCAGGUGCAGGCCCAGUUGU---
Oryctolagus cuniculus        GUGACCGGGUCUGCUGAGUCCGCAGCACUCAGACUACGUGCAUC--UGCAGCAGGUGCAGGCCCAGCUGU---
Xenopus laevis               GAGACCGGGUCCGCUGAGUCCGCAGCACUCAGACUAUGUGCCCCUCUGCAGCAGGAGCAGGCCCAGAUGU---
Takifugu rubipres            GGGGUCGGGUCUUCUGAGUCCGCAGCACUCAGGCUACGUGUGCCUCCGCAGCAGGUGCAGGCCCAG-------
Danio rerio                  GUGACCGGGUCUUCUGAGUCCGCAGCACUCAGGCUACGUGUGCCUCCGCAGCAGGUGCAGGCCCAG-------
Saimiri boliviensis          GUGACCGGGUCUGCUGAGUCCGCAGCACUCAGACUACGUGCACCUCUGCAGCAGGUGCAGGCCCAGUUGU---
Mus musculus                 GUGGCCGGGUCUGCUGAGUCCGCAGCACUCAGACUAUGUGCACCUCUGCAGCAGGUGCAGGCCCAGUUGU---
Homo sapiens                 GUGGCCGGGUCUGCUGAGUCCGCAGCACUCAGACUACGUGCACCUCUGCAGCAGGUGCAGGCCCAGUUGU---
Pteropus alecto              GUGGCCGGGUCUGCUGAGUCCGCAGCACUCAGACUACGUGCACCUCUGCAGCAGGUGCAGGCCCAGUUGU---
Mesocricetus auratus         GUGGCCGGGUCUGCUGAGUCCGCAGCACUCAGACUACGUGCACCUCUGCAGCAGGUGCAGGCCCAGUUGU---
Tursiops truncatus           GUGGCCGGGUCUGCUGAGUCCGCAGCACUCAGACUACGUGCACCUCUGCAGCAGGUGCAGGCCCAGUUGU---
Nomascus leucogenys          GUGGCCGGGUCUGCUGAGUCCGCAGCACUCAGACUACGUGCACCUCUGCAGCAGGUGCAGGCCCAGUUGU---
Gorilla gorilla gorilla      GUGGCCGGGUCUGCUGAGUCCGCAGCACUCAGACUACGUGCACCUCUGCAGCAGGUGCAGGCCCAGUUGU---
Ovis aries                   GUGGCCGGGUCUGCUGAGUCCGCAGCACUCAGACUACGUGCACCUCUGCAGCAGGUGCAGGCCCAGUUGU---
Macaca mulatta               GUGGCCGGGUCUGCUGAGUCCGCAGCACUCAGACUACGUGCACCUCUGCAGCAGGUGCAGGCCCAGUUGU---
Bos taurus                   GUGGCCGGGUCUGCUGAGUCCGCAGCACUCAGACUACGUGCACCUCUGCAGCAGGUGCAGGCCCAGUUGU---
Papio anubis                 GUGGCCGGGUCUGCUGAGUCCGCAGCACUCAGACUACGUGCACCUCUGCAGCAGGUGCAGGCCCAGUUGU---
Pan paniscus                 GUGGCCGGGUCUGCUGAGUCCGCAGCACUCAGACUACGUGCACCUCUGCAGCAGGUGCAGGCCCAGUUGU---
Pongo abelii                 GUGGCCGGGUCUGCUGAGUCCGCAGCACUCAGACUACGUGCACCUCUGCAGCAGGUGCAGGCCCAGUUGU---
Pan troglodytes              GUGGCCGGGUCUGCUGAGUCCGCAGCACUCAGACUACGUGCACCUCUGCAGCAGGUGCAGGCCCAGUUGU---
Cricetus griseus             GUGGCCGGGUCUGCUGAGUCCGCAGCACUCAGACUACGUGCACCUCUGCAGCAGGUGCAGGCCCAGUUGU---
Sus scrofa                   GUGGCCGGGUCUGCUGAGUCCGCAGCACUCAGACUACGUGCACCUCUGCAGCAGGUGCAGGCCCAGUUGU---
Rattus norvegicus            GUGGCCGGGUCUGCUGAGUCCGCAGCACUCAGACUACGUGCGCCUCUGCAGCAGGUGCAGGCCCAGUUGU---
Gallus gallus                GUGACCGGGUCCGCUGAGUCCGCAGCACUCAGACUACGUGUUCCUCUGCAGCAGGUGCAGGCCCAGCUGU---
Pseudopodoces humilis        GUGACCGGGUCCGCUGAGUCCGCAGCACUCAGACUACGUGUUCCUCUGCAGCAGGUGCAGGCCCAG-------
Zonotrichia albicollis       GUGACCGGGUCCGCUGAGUCCGCAGCACUCAGACUACGUGUUCCUCUGCAGCAGGUGCAGGCCCAG-------
Chrysemis picta belli        GUGACCGGGUCCGCUGAGUCCGCAGCACUCAGACUACGUGUUCCUCUGCAGCAGGUGCAGGCCCAG-------
Melopsittacus undulatus      GUGACCGGGUCCGCUGAGUCCGCAGCACUCAGACUACGUGUUCCUCUGCAGCAGGUGCAGGCCCAG-------
Ficedula albicollis          GUGACCGGGUCCGCUGAGUCCGCAGCACUCAGACUACGUGUUCCUCUGCAGCAGGUGCAGGCCCAG-------
Anas platyrhynchos           GUGACCGGGUCCGCUGAGUCCGCAGCACUCAGACUACGUGUUCCUCUGCAGCAGGUGCAGGCCCAG-------
Alligator mississippiensis   GUGACCGGGUCCGCUGAGUCCGCAGCACUCAGACUACGUGCUCCUCUGCAGCAGGCGCAGGCCCAG-------
Alligator sinensis           GUGACCGGGUCCGCUGAGUCCGCAGCACUCAGACUACGUGCUCCUCUGCAGCAGGCGCAGGCCCAG-------
                             *    *        **  ** ****** **       **   *   ** * **       *
```

B

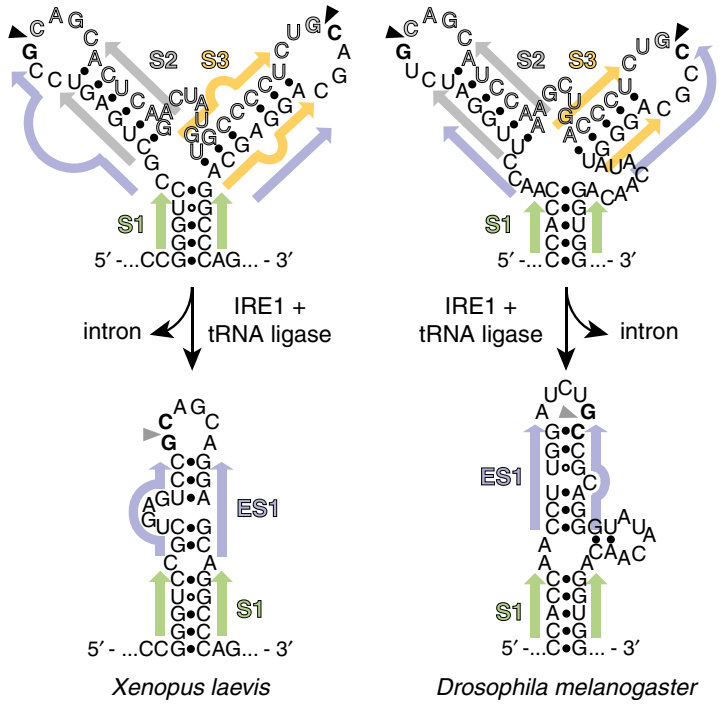

C

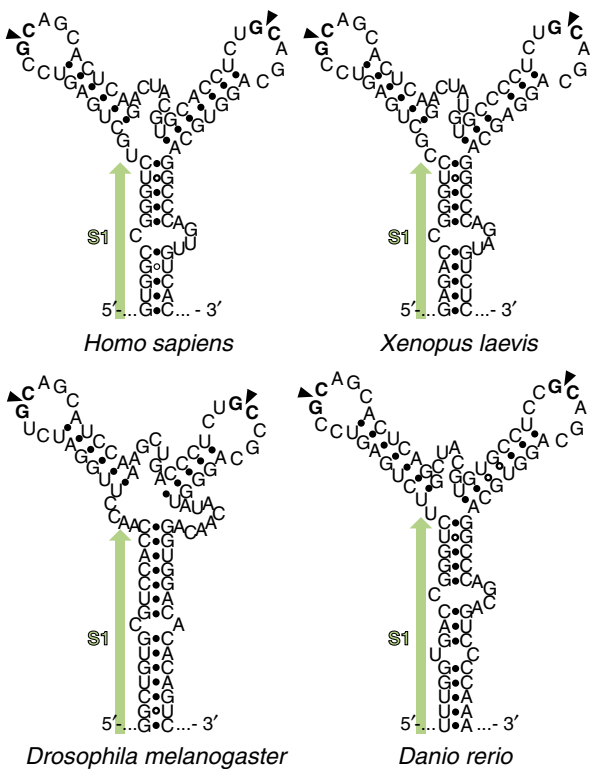

Figure EV1.

Figure EV1. Evolutionary conservation of sequence and structural features of *XBP1*-BSL.

A Multiple sequence alignment of *XBP1*-BSL from phylogenetically diverse metazoans. Grey boxes: 7-mer loops harboring the conserved cleavage sites. Dash-outlined box: *XBP1* intron.

B Secondary structures of select sequences in (A), and their corresponding spliced RNAs. Arrowheads: scissile bonds (unspliced structure); exon–exon junction (spliced structure). Closed circles: Watson–Crick base pairs. Open circles: Wobble base pairs. Colored arrows: stems in unspliced or spliced *XBP1*-BSL structures. S1, central stem; S2, S3, arm stems; ES1 extended stem.

C Secondary structures of select sequences in (A) showing the extension of S1.

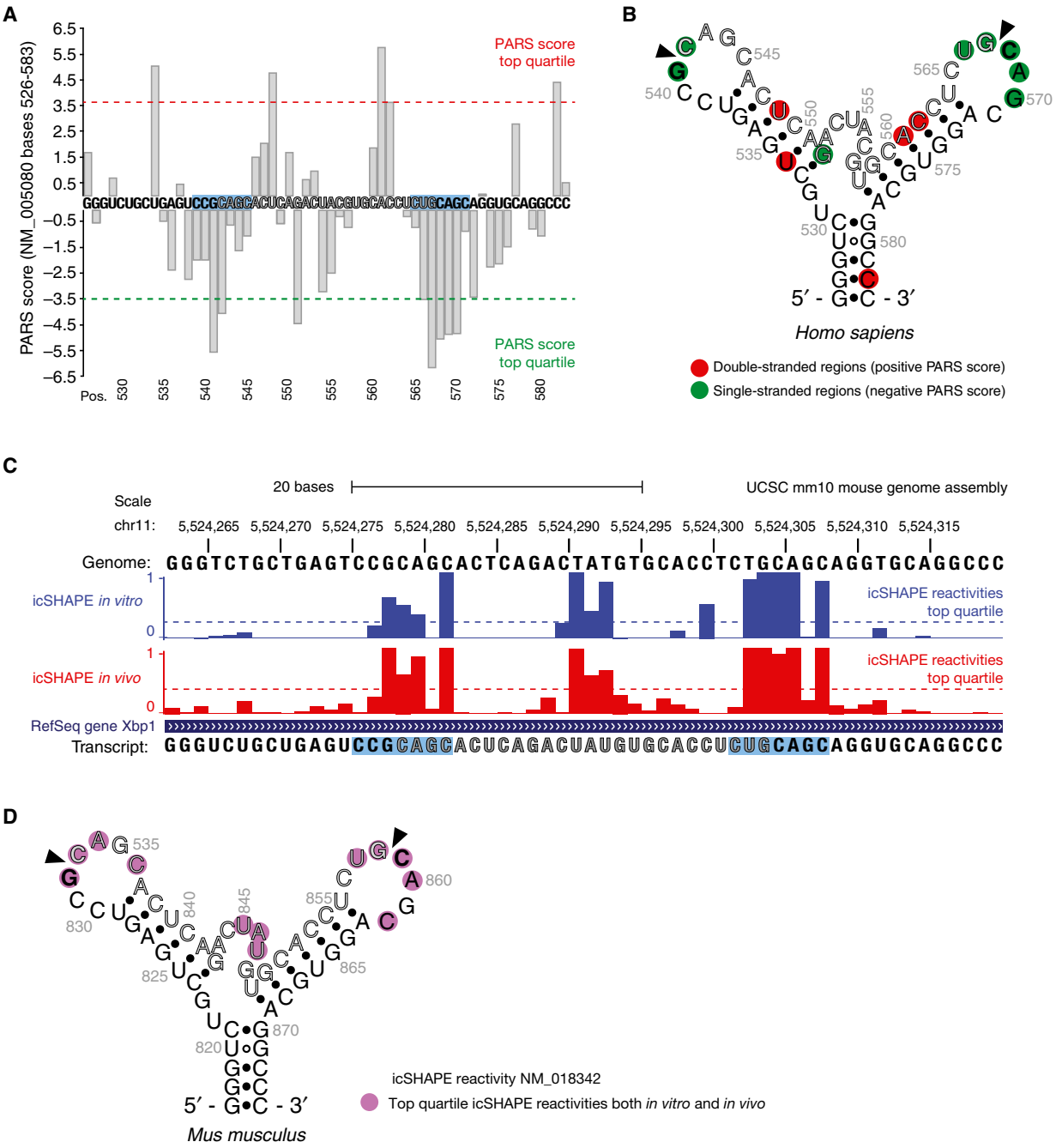

Figure EV2.

Figure EV2. *In vivo* structure of *XBP1*-BSL.

A Parallel analysis of RNA structure (PARS) performed on the transcript encoding unspliced *XBP1* mRNA of human origin (NCBI Accession NM_005080). Data were obtained from the Gene Expression Omnibus accession GSE50676. Nuclease digestion profiles for RNase V1 (cleaving double-stranded RNA) and S1 nuclease (cleaving single-stranded RNA) after deep-sequencing are combined to generate a PARS score, defined as the ratio of mapped reads obtained from RNA libraries prepared after digestion with either nuclease [22]. PARS scores for nucleotides at positions 526–583 are shown. The cut-off values for the PARS scores corresponding to the top quartile (most significant) are indicated. The intron is colored in grey. The blue boxes indicate the 7-mer loop harboring the IRE1 cleavage site.

B Secondary structure of the region corresponding to the nucleotides shown in (A). Colored circles indicate the corresponding PARS score per position.

C UCSC Genome Browser view showing the RNA secondary structure signature of *Xbp1* mRNA of mouse origin as determined by *in vivo* click selective 2′-hydroxyl acylation and profiling experiments (icSHAPE). The bar graphs indicate the icSHAPE reactivities reported in the Gene Expression Omnibus accession GSE64169 for the corresponding transcript (NCBI Accession NM_018342). Cutoff values for the icSHAPE reactivity values corresponding to the top quartile (most significant) are indicated. The intron is colored in grey. The blue boxes indicate the 7-mer loop harboring the IRE1 cleavage site.

D Secondary structure of the region corresponding to the nucleotides 817–874 of the transcript shown in (C). Colored circles indicate the corresponding icSHAPE reactivity value above the top quartile threshold per position.

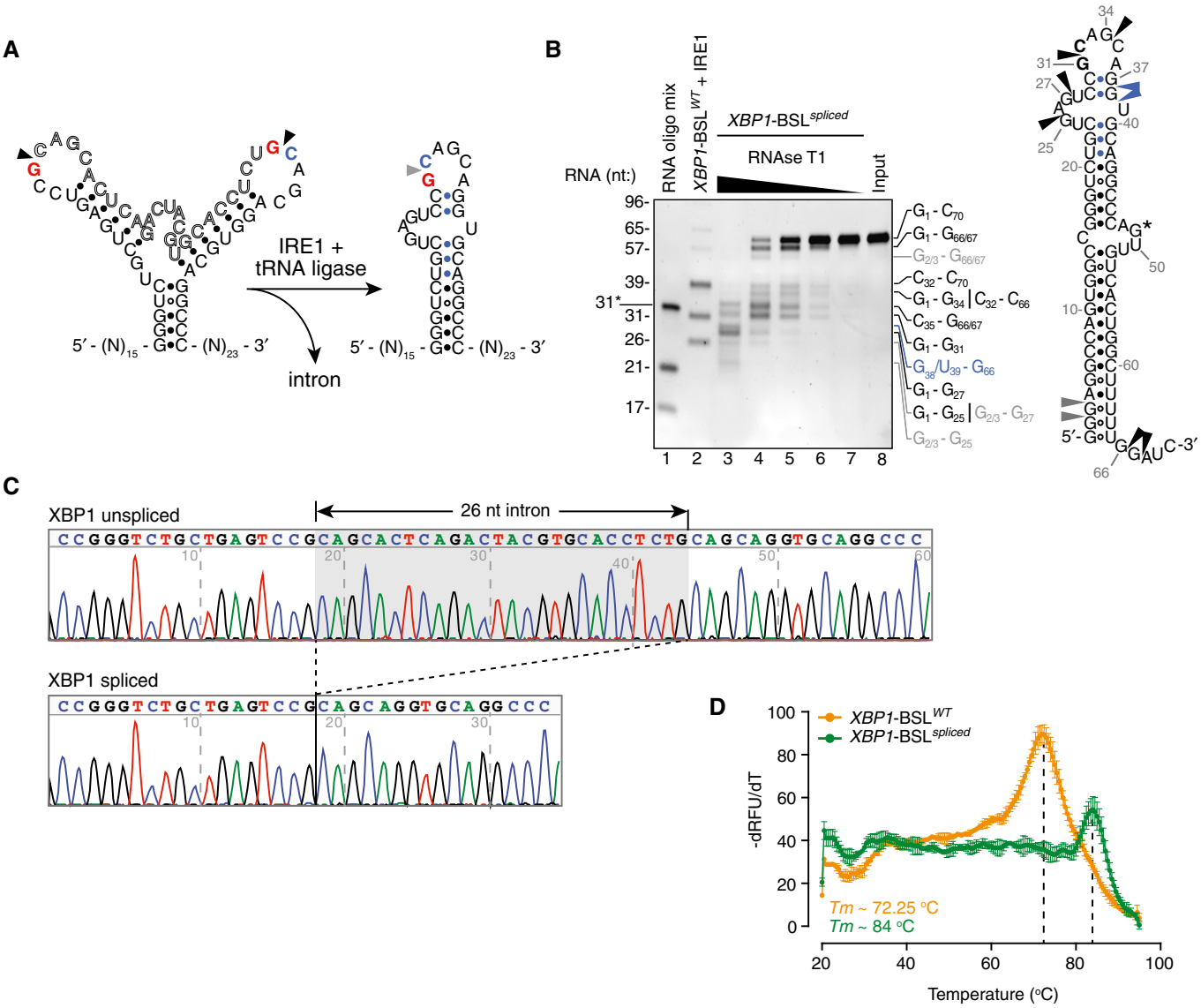

Figure EV3.

Figure EV3. Biochemical analysis of the *XBP1* splicing product.

A Secondary structures of the short RNA transcripts harboring the human *XBP1*-BSL (left structure) or its corresponding spliced RNA (right structure). Arrowheads: scissile bonds (unspliced structure); exon–exon junction (spliced structure). The exon boundaries are indicated by a red guanosine, a blue cytosine. Blue closed circles: Watson–Crick base pairing between the 5′ and 3′ exons that form ES1.

B Left: TBE–urea gel showing the ribonuclease T1 (RNase T1) mapping of the *XBP1*-BSL^{spliced} RNA. RNA ladders: RNA oligo mix (lane 1), and IRE1-cleaved *XBP1*-BSL^{WT} (lane 2). 31* indicates the migration of a 2′-ACE-(acid-labile orthoester)-protected RNA oligonucleotide. The *XBP1*-BSL-derived RNA ladder was cleaved with 0.5 μM of IRE1α-KR43. The fragments generated by RNase T1 are indicated on the right side of the gel and color coded according to their origin (see schematic). Right: schematic of the *XBP1*-BSL^{spliced} transcript. Blue: closed circles: Watson–Crick base pairs between the 5′ and 3′ exons that form ES1. Black arrowheads: preferred cleavage sites by RNase T1. Blue arrowheads: overdigestion products generated when the distal C-G pairs of ES1 are melted. Grey arrowheads: possible cleavage products resulting from the melting of G-U wobble base pairs at the beginning of the main stem S1. G* indicates a single inaccessible single-stranded guanosine.

C Electropherograms showing the sequencing analysis of *in vitro*-generated splice products using *XBP1*-BSL^{WT} as a substrate.

D Melting curves of the *XBP1*-BSL^{WT} or *XBP1*-BSL^{spliced} RNA transcripts. The melting curve analysis is consistent with the faster-than-expected mobility of the spliced RNA in TBE–urea–PAGE gels (this RNA migrates faster than its predicted molecular size of 70 nt, see B), which suggests it is partially denatured during TBE–urea–PAGE electrophoresis. Mean ± SD.

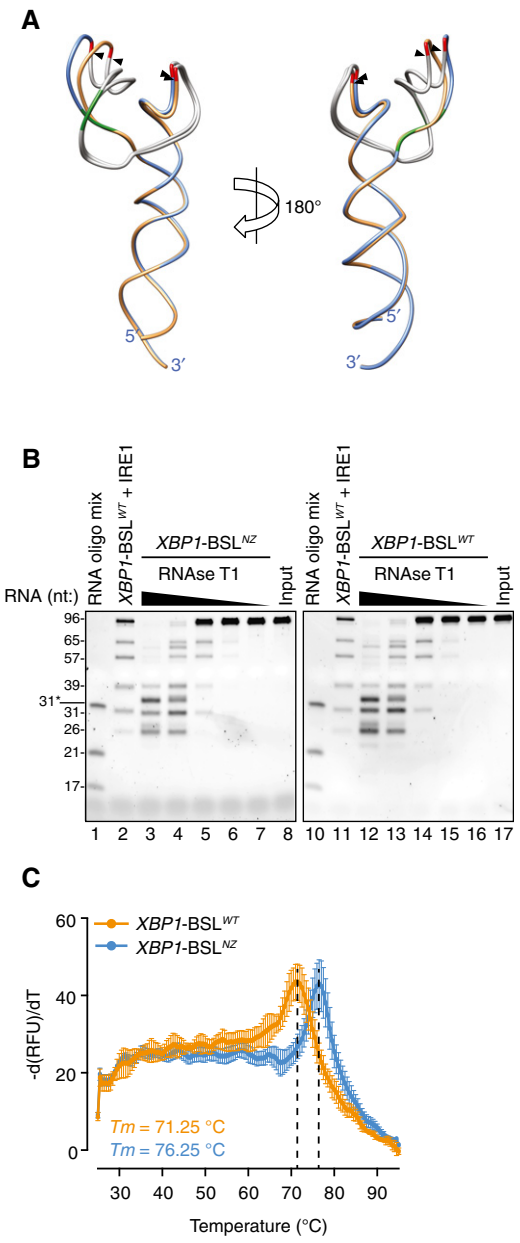

Figure EV4. The non-zipper mutant of *XBP1*-BSL does not disrupt the secondary structure.

A Superimposition of the predicted tertiary structures of the non-zipper mutant *XBP1*-BSL^{NZ} (exons colored in blue, ΔG = −43.60 kcal/mol), and the corresponding wild-type *XBP1*-BSL (exons colored in gold, ΔG = −43.10 kcal/mol) RNAs used in this study. Arrowheads: scissile bonds. The intron is colored in grey. The guanosines 3′ of the scissile bond are colored in red. Mutant bases that disrupt the exon–exon base pairing after cleavage are colored in green.

B TBE–urea gels showing the RNase T1 mapping of the *XBP1*-BSL^{NZ} or *XBP1*-BSL^{WT} RNAs. RNA ladders: RNA oligo mix (lanes 1 and 10), and IRE1-cleaved *XBP1*-BSL^{WT} (lanes 2 and 11). 31* indicates the migration of a 2′-ACE-(acid-labile orthoester)-protected RNA oligonucleotide. The *XBP1*-BSL-derived RNA ladder was cleaved with 0.5 μM of IRE1α-KR43.

C Melting curves of the *XBP1*-BSL^{WT} or *XBP1*-BSL^{NZ} RNA transcripts. Mean ± SD.

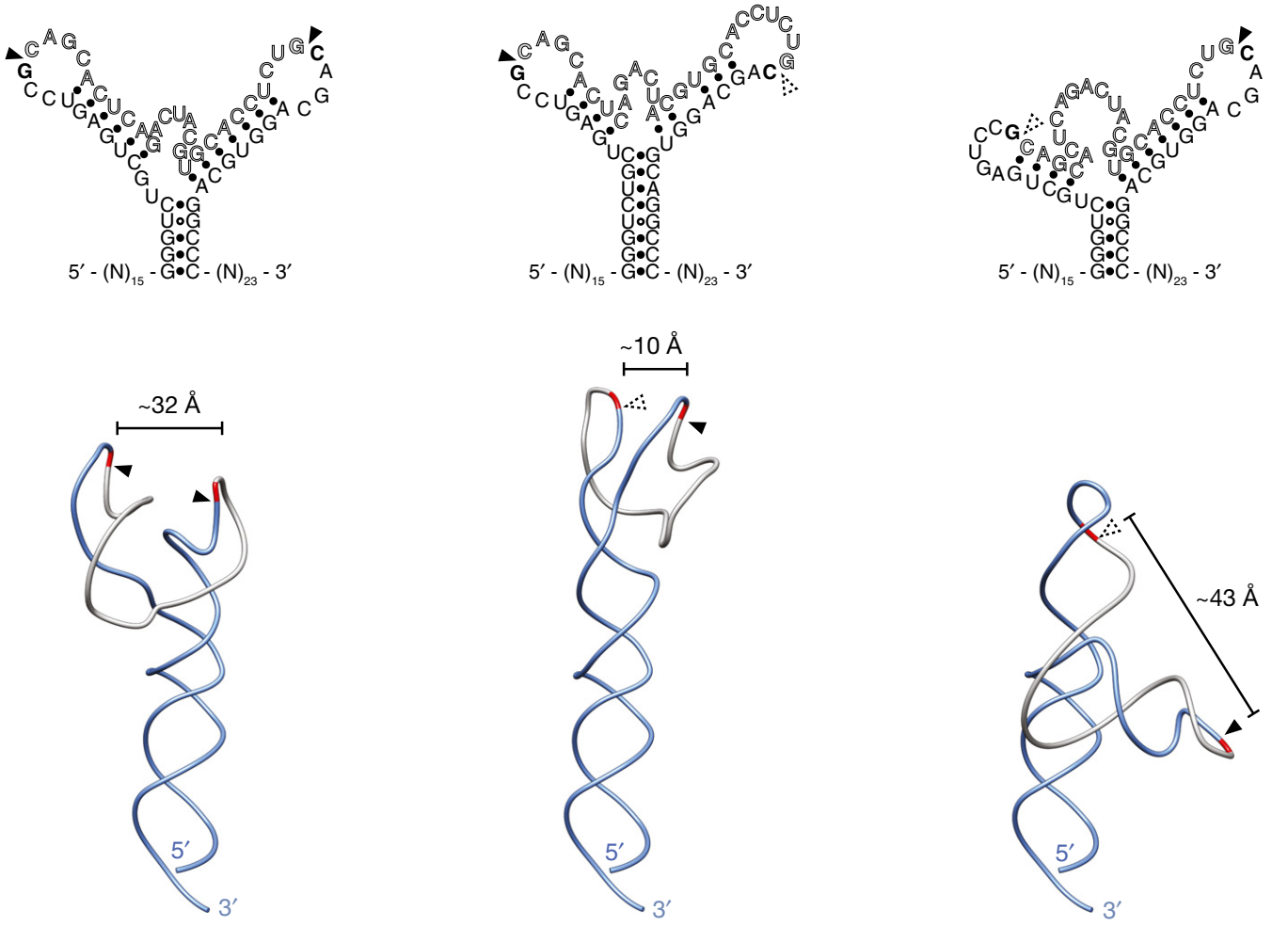

Figure EV5. Alternative secondary structures for *XBP1*-BSL.
Predicted secondary (top) and tertiary (bottom) structures of the wild-type human *XBP1*-BSL RNA probe used throughout this study. Arrowheads: scissile bonds. Calculated distances between scissile bonds are indicated. Dashed arrowheads: scissile bonds placed in a context distinct from the 7-mer loop recognized by IRE1.